Statistical analysis and treatment method of head checks on the Belgian railway network

Vernaillen, Tim; Zhang, Pan; Núñez, Alfredo; Dollevoet, Rolf; Li, Zili

DOI
10.1016/j.ijfatigue.2025.109349

Publication date
2025

Document Version
Final published version

Published in
International Journal of Fatigue

International Journal of Fatigue 203 (2026) 109349

Contents lists available at ScienceDirect

International Journal of Fatigue

journal homepage: www.elsevier.com/locate/ijfatigue

Statistical analysis and treatment method of head checks on the Belgian railway network

Tim Vernaillen [a,b], Pan Zhang [a,*], Alfredo Núñez [a], Rolf Dollevoet [a], Zili Li [a,*]

[a] Section of Railway Engineering, Delft University of Technology, Stevinweg 1, 2628CN Delft, the Netherlands
[b] Infrabel, Place Marcel Broodthaers 2, 1060 Brussels, Belgium

ARTICLE INFO

Keywords:
Rolling contact fatigue
Head checks
Crack growth
Eddy current
Rail grinding
Magic wear rate

ABSTRACT

This paper investigates the growth and treatment of a major type of rail rolling contact fatigue (RCF) known as head checks (HCs). The analysis is based on extensive field data of 212 curved tracks made of R260 steel across the entire Belgian railway network. The HC crack depth was mainly measured by eddy current testing. The growth rates of HCs are analysed in relation to the curve radius, annual traffic load, and rail wear. The key findings are as follows: 1) Tracks with radii between 750 and 1000 m exhibit the highest HC growth rate of about 1.5 mm per 100 million gross tons (MGT) and the largest occurrence probability of about 25 %. 2) A counter-intuitive result is that the HC growth per MGT is higher on lines with lower annual traffic loads, consistent with the trend observed in rail wear rates. 3) The artificial wear methods to control RCF, such as preventive grinding, should consider annual traffic load and service time, rather than solely accumulated tonnage, as is the current practice. Based on these findings, a new method is proposed to estimate the magic wear rate for the Belgian railways, which can serve as input for optimising grinding operations to mitigate HCs.

1. Introduction

Rail defects caused by rolling contact fatigue (RCF) pose an increasing challenge to the railway industry worldwide [1–3]. They are a significant factor driving the cost of rail maintenance and renewal, and are expected to occur more frequently due to growing demands for rail services. Head checks (HCs) are a major type of RCF defect, characterised by clusters of inclined, closely spaced cracks in the rail shoulder or gauge corner [4,5]. Infra managers of railway networks worldwide have implemented various strategies to detect [6], assess [7], mitigate, and prevent HCs [8–10]. Since 2015, Infrabel, the Belgian rail infrastructure manager, has experienced a steady annual rise in maintenance costs related to HCs, including the need for additional testing, preventive grinding, corrective milling, and rail renewal. To better control the life cycle cost for rails, there is an urgent need to develop more effective treatment methods for HCs, on the basis of a deeper understanding of the HC development.

HCs typically occur on the outer rails of curves with radii between 500 m and 3000 m [11]. Previous studies have investigated the initiation and growth of HCs through numerical simulations [12–15], laboratory tests [16–18] and field monitoring [19–21]. On curved tracks, the wheel flange frequently contacts the shoulder or gauge corner of the outer rail due to the angle of attack and centrifugal forces of the train. The resulting lateral and spin creepages, combined with the possible longitudinal creepage from traction or braking, generate high shear stresses at the wheel-rail interface. These stresses cause cyclic plastic deformation of rail materials, triggering the initiation of HCs [12,22,23]. Once initiated, cracks can propagate deeper into the rail material, a process accelerated by tractive forces [14] and fluid entrapment within cracks [24–26]. While existing research predominantly investigates HC formation under specific loading conditions on particular track sections, large-scale statistical analyses of HC growth across entire railway networks remain scarce.

Several countermeasures have been applied to mitigate HCs, such as anti-stress rail profile [11,27], lubrication [28], and rail grinding [29]. Among these, preventive grinding is widely used in practice, with grinding intervals often based on accumulated tonnage. However, the growth of HCs is influenced not only by total accumulated tonnage but also by various parameters, including curve radius, steel grade, and wear [21]. Therefore, effective preventive grinding strategies must account for these operational complexities and diverse track parameters and conditions. The optimal grinding interval should achieve a balance

* Corresponding authors.
E-mail addresses: zhang.tudelft.994@gmail.com (P. Zhang), z.li@tudelft.nl (Z. Li).

https://doi.org/10.1016/j.ijfatigue.2025.109349
Received 24 July 2025; Received in revised form 29 September 2025; Accepted 25 October 2025
Available online 27 October 2025

between adequately preventing RCF defects and avoiding excessive grinding that can shorten rail life. This concept aligns with the concept of the 'magic' wear rate (MWR), which represents the practical balance between wear and RCF damage on rails [30,31]. The MWR represents an optimal combination of natural and artificial material removal that effectively controls rolling contact fatigue without unnecessarily accelerating rail degradation. To the best knowledge of the authors, the MWR for HCs treatment has not yet been defined quantitatively, highlighting the need for large-scale comprehensive analyses of entire railway networks to account for the different HC growth rates under complex operational conditions.

This paper aims to enhance the understanding of HC growth by a statistical analysis. To achieve this goal, an extensive investigation was carried out on HCs from 212 curved track sections across the whole Belgian railway network, covering various track curvatures and train loading conditions. Based on this analysis, a more effective HC treatment approach using preventive grinding and MWR is proposed. The structure of this paper is organised as follows. Section 2 describes the field conditions, development phases, and assessment methods of HCs. Section 3 presents and discusses the HC growth rates in relation to the curve radius, accumulated tonnage, annual traffic, and rail wear. Section 4 evaluates the effectiveness of the current grinding policy on controlling HCs and proposes an optimal grinding strategy, i.e., an MWR for the Belgian network. The main conclusions are summarised in Section 5.

2. Field monitoring methods of HCs

This section first introduces the typical development phases of HCs and the nondestructive testing methods used for their detection. Afterwards, we take the HCs in the Belgian railway network for the case study and describe the quantitative assessment methods of HC growth rates.

2.1. Development phases and detection methods of HCs

In general, the development of HCs can be divided into three phases, following the empirical approach proposed in [21]. Fig. 1 shows some typical HC cracks observed in the Belgian railway network. Phase I is the initial crack formation with depths smaller than 0.1 mm, typically during the first 5–10 MGT of traffic. In Phase II (depth between 0.1 and 5.0 mm), HCs show a relatively low and uniform crack growth into the rail at a shallow angle of approximately 15–30°, with a typical rate of around 1.0 mm/100 MGT in the vertical direction [21]. In this phase, corrective maintenance by grinding or milling could be performed for HC treatment. In Phase III (depth larger than 5.0 mm), cracks develop horizontally with vertical branches at a considerably fast growth rate up to 1 mm/ 1 MGT [21], and thus, they are rather short-duration events. In this phase, corrective maintenance is not possible, and rail replacement is almost inevitable to avoid rail breakage. Figs. 1e and 1f show two examples of the further rail degradation due to HCs. It is important to note that this empirical classification is derived from a large field database and intended to reflect general trends in HC development. It may not capture the full complexity of individual crack formation processes.

Two nondestructive testing methods are usually used to detect the rail cracks: the eddy current testing (ECT) and the ultrasonic testing (UT) methods. The ECT is sensitive to the conditions at the rail surface [32], and is suitable to detect clusters of HC cracks in Phase II with depths from 0.1 to 5.0 mm. The UT mainly detects local and deep cracks, which can be used to measure the dangerous transverse defects of HC cracks in Phase III above 5.0 mm. The HC cracks in Phase I may begin to appear visually to the naked eye, but they are below the detection threshold of both ECT and UT systems.

2.2. HCs in the Belgian railway network

By 2000, HCs were registered by visual inspection on the Belgian rail network. Afterwards, UT on a dedicated test vehicle was employed in the entire network for HC detection, as shown in Fig. 2a. However, UT mainly measures moderate and severe cracks, e.g., with depths more than 5.0 mm, and cannot identify the small HCs in the early stage. It is reported that the number of rail breaks due to HCs increased from 0 in 2010 to 12 in 2014. Therefore, since 2014, the ECT system has been installed in the test vehicle to detect HCs. This system consists of ten vertical spring-loaded probes across the full width of the rail head (see Fig. 2b), to detect vertical crack depth (see Fig. 2c) ranging from 0.1 to 5.0 mm. Data collected from all ten probes were at 1 mm intervals along the track, with a depth resolution of 0.1 mm. The ECT and UT in Belgium used a commercial system provided by Sperry, operating at speeds of up

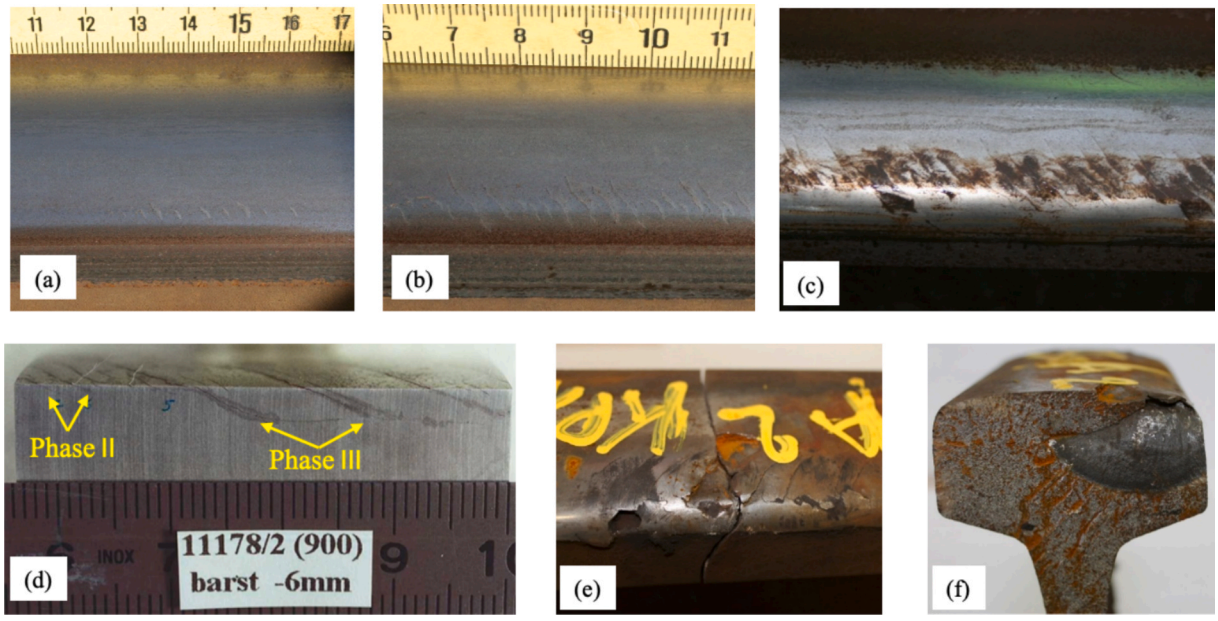

Fig. 1. Different development phases of HCs in the Belgian railway network. (a) Phase I: initial crack formation; (b) Phase II: uniform crack growth into the rail; (c) Phase III: cracks develop horizontally with vertical branches, with a significant rise in the crack growth rate; (d) a cross-section of Phases II and III HCs along the middle of the running band (not the same rail as in (c)); (e) Rail surface breakage due to HCs; (f) Transverse HC fatigue crack of Phase III.

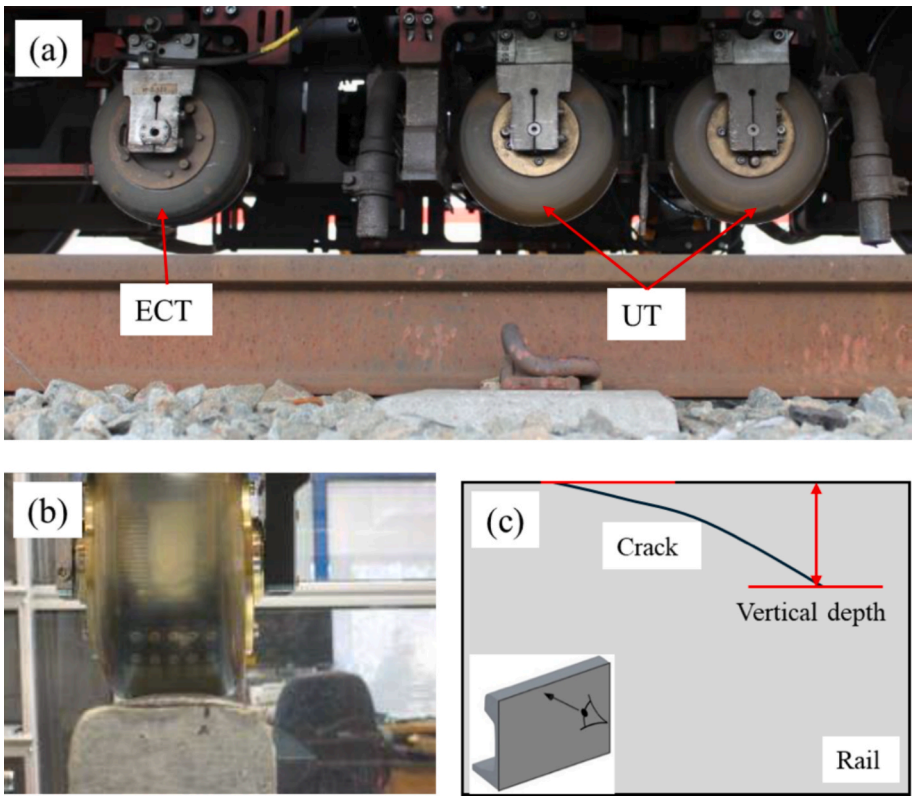

Fig. 2. Field ECT and UC systems in a dedicated test vehicle in Belgium. (a) The test vehicle; (b) the ECT system; (c) a schematic drawing of the HC depth measurement by ECT.

to 50 km/h. This system is designed to operate reliably across a wide range of environmental and operational conditions, and has been widely deployed in many countries including Belgium, the UK, Germany, the United States, and China. The reported inspection accuracy ranges between 85 % and 95 %, depending on track conditions.

To prevent HCs, Infrabel launched a cyclic grinding program on UIC classes 1 to 4 lines (defined below in Equation (1) [33], TL_i refers to the measured traffic load for track Section i) in 2012, which implied a rail removal of 0.25 mm per 80 MGT on both curves and tangent tracks. This was found to be insufficient to avoid HCs. Since 2016, the grinding strategy has been changed to 0.25 mm per 60 MGT on tangent tracks and 0.25 mm per 25 MGT in curves for all UIC classes 1 to 6. This program results in a decrease in HCs of both Phase II (375 km with HCs in 2016 compared to 125 km in 2023) and Phase III (411 new individual cracks from UT in 2014 compared to 38 in 2022). We also observe a significant reduction in the number of rail breaks caused by HCs, which is 12 in total from April 2014 to March 2015, compared to 1 from April 2022 to March 2023.

$$\mathrm{UIC}_i = \begin{cases} UIC1 if 130000[ton/day] < \mathrm{TL}_i \\ UIC2 if 80000[ton/day] < \mathrm{TL}_i \le 130000[ton/day] \\ UIC3 if 40000[ton/day] < \mathrm{TL}_i \le 80000[ton/day] \\ UIC4 if 20000[ton/day] < \mathrm{TL}_i \le 40000[ton/day] \\ UIC5 if 5000[ton/day] < \mathrm{TL}_i \le 20000[ton/day] \\ UIC6 if \mathrm{TL}_i \le 5000[ton/day] \end{cases} \quad (1)$$

The analysis in this work was mainly based on the extensive field data across the entire Belgian network in 2019. The curves of R260 rails with radii smaller than 3000 m were considered, amounting to a total of 1429 km among the 3113 km of measured tracks. For these curves, the grinding interval was 0.25 mm/80 MGT between 2012 and 2016, and has been 0.25 mm/25 MGT since 2016. It is worth noting that from 2012 to 2019, some lines might have undergone less grinding than others in practice, due to the initial trial and implementation of preventive grinding programs during these periods, such as for UIC 4 lines [33]. Only HCs in Phase II, as detected by ECT, were analysed, since their slow and uniform crack growth makes it reasonable to define an average growth rate for them. This analysis covered 212 curves with a total length of 172 km. These rails are on conventional railway lines with mixed passenger and freight traffic, excluding high-speed and freight lines. Two rail profiles are used: the UIC60E1 profile and the Belgian 50E2 profile according to the standard EN 13,674–1 [33]. These two profiles have different geometrical dimensions, but the same nominal curvature across the rail head, including gage corner and the same rail head width, and thus the same wheel-rail contact geometries. The rail inclinations were both 1:20, with a nominal track gauge of 1435 mm. The complete network was measured twice a year with the vehicle EM130 to record the track parameters every 25 cm, such as the longitudinal and vertical profiles and rail cant. Another dedicated vehicle equipped with UT and ECT measurement systems was used to detect cracks twice a year.

2.3. Assessment methods of HCs

This work mainly analyses the influence of the track radius and annual tonnage on the growth rates of HCs. Fig. 3a shows the locations of the 212 curves with HCs across the Belgian railway network, indicated by the red lines. The average HC depth $h_{t,c}$ in each is defined as follows,

$$h_{t,c} = \frac{1}{x_{t,c}^{\mathrm{end}} - x_{t,c}^{\mathrm{ini}}} \sum_{j=x_{t,c}^{\mathrm{ini}}}^{x_{t,c}^{\mathrm{end}}} \max_{p\in\{1,\ldots,P\}} d_{t,c,j,p} \quad (2)$$

where $d_{t,c,j,p}$ is the vertical depth measured by probe p at kilometre position point j of the curve c (c = 1, 2,…., 212) in year t, P is the total number of probes (P = 10), and $x_{t,c}^{\mathrm{ini}}$ and $x_{t,c}^{\mathrm{end}}$ are the kilometre position points in curve c where the head check defect is first detected and

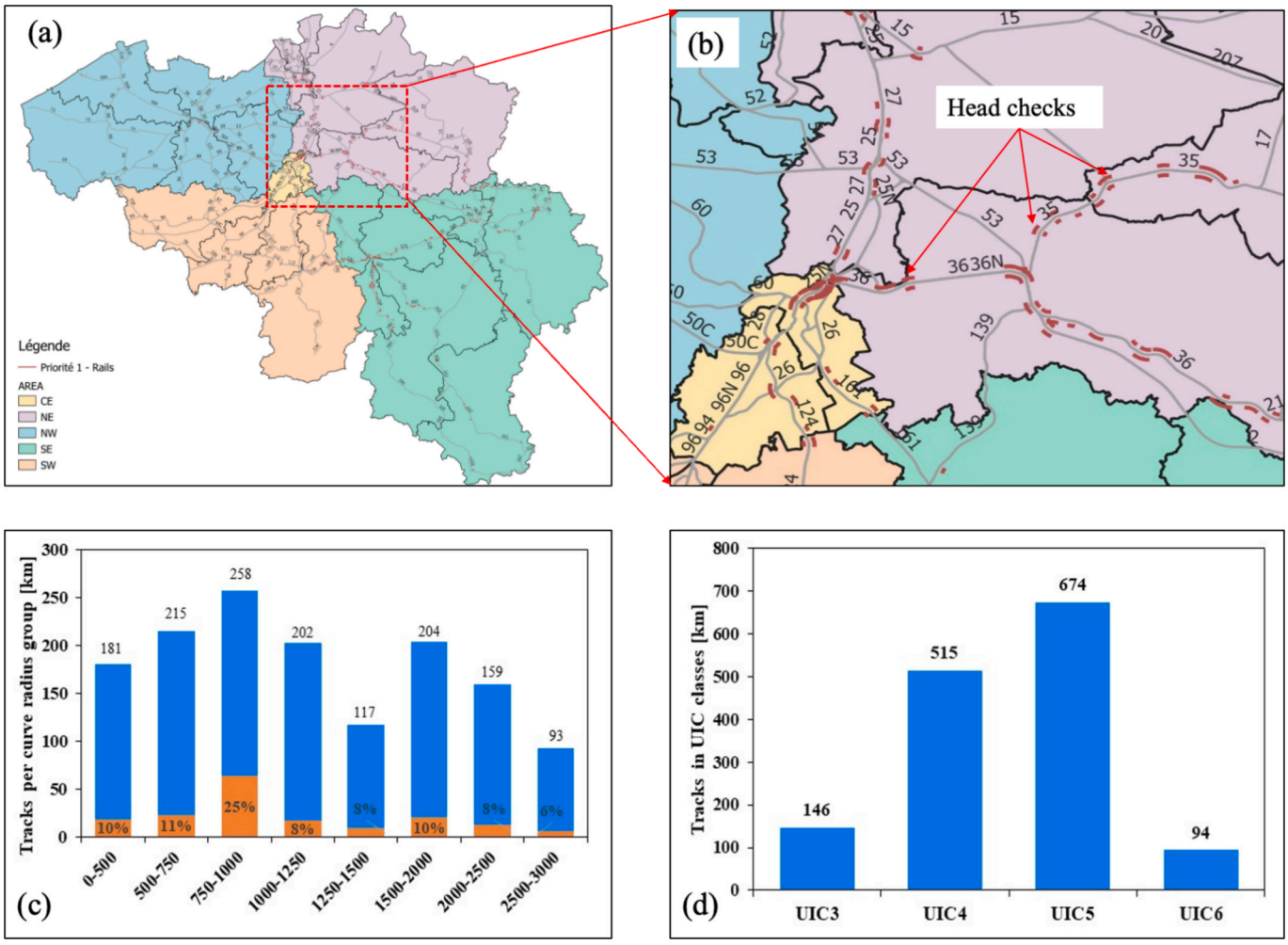

Fig. 3. Statistical data of HCs in the Belgian rail network. (a) The analysed curved tracks with HCs across the entire Belgian rail network; (b) zoom-in of a certain area of (a); (c) the total mileage of tracks per curve radius group in blue, with the percentage of tracks with HCs in orange. (d) division of the analysed curves into UIC classes.

where it ends in the measurement campaign conducted in year t.

The HC growth rate per 100 MGT is defined as follows,

$$\Delta h^{\mathrm{T}}_{t,c} = \frac{100 h_{t,c}}{A_t (t - t_0)} \tag{3}$$

where $\Delta h^{\mathrm{T}}_{t,c}$ is the HC growth rate of curve c per 100 MGT (mm/100 MGT) in year t, $h_{t,c}$ in mm is the average defect depth of curve c measured in year t, A_t is the average annual traffic load in MGT in the years between t_0 and t, and t_0 is the year of the rail installation. It is worth noting that the measured HC growth rate represents the residual or net crack growth, i.e., the portion of crack growth that remains after accounting for the rail wear. Mathematically, the total crack growth would be approximately the sum of the measured crack growth and the material removed through wear.

The HC growth rate per year since the installation of the rails is calculated as follows:

$$\Delta h^{\mathrm{Y}}_{t,c} = \frac{h_{t,c}}{t - t_0} \tag{4}$$

where $\Delta h^{\mathrm{Y}}_{t,c}$ is the HC growth rate per year in mm/year measured in year t.

The track curve radius is divided into the following eight groups:

$$R_i = \begin{cases} 1 & \text{if} \quad R \le 500\text{m} \\ 2 & \text{if} \quad 500\text{m} \le R \le 750\text{m} \\ 3 & \text{if} \quad 750\text{m} \le R \le 1000\text{m} \\ 4 & \text{if} \quad 1000\text{m} \le R \le 1250\text{m} \\ 5 & \text{if} \quad 1250\text{m} \le R \le 1500\text{m} \\ 6 & \text{if} \quad 1500\text{m} \le R \le 2000\text{m} \\ 7 & \text{if} \quad 2000\text{m} \le R \le 2500\text{m} \\ 8 & \text{if} \quad 2500\text{m} \le R \le 3000\text{m} \end{cases} \tag{5}$$

where R_i is the number of a curve radius group where track segment i belongs, and R is the measured radius. Fig. 3b presents the total mileages of tracks per curve radius group (in blue) and the percentage of tracks with HCs (in orange). All track sections are also assigned to a specific UIC class depending on the annual MGT, as shown in Fig. 3c. Given the negligible track length in the UIC1 and UIC2 classes, they are not considered in this analysis. All the measurements from different databases and measuring vehicles were merged into a single data set and averaged per 50 m, for the same rail grade, profile, curve radius and annual tonnage. The transition curves are also included and averaged per 50 m.

3. Results and discussions of HC growth rates

In this section, the growth rate of HCs in Phase II is analysed with different track radii and traffic loads. The relationship between HC

growth and rail wear is also investigated.

3.1. HC growth rate versus track radius

Fig. 4 shows the HC growth rates of R260 rails in relation to the track radius, based on statistical data from all 212 curves measured in 2019. It can be seen that the HC growth rate initially increases from about 1.0 mm/100 MGT for curves with radii of 0–500 m, reaching a peak at 1.5 mm/100 MGT in the 750–1000 m range. Afterwards, the growth rate gradually declines with increasing track radius, and reaches a minimum of about 0.4 mm/100 MGT for curves with radii between 2500–3000 m. Combined with Fig. 3b, it is found that curves with radii between 750–1000 m have not only the highest HC growth rates, but also the largest HC occurrence probability (25 %), in contrast to only 6 %-11 % on the other curves.

The variation trend of HC growth rates with respect to the curve radius can be qualitatively explained by the competing mechanisms between wear and RCF [19,34,35]. In curves with relatively smaller radii, the friction energy is generally higher, promoting the development of RCF defects. This explains the overall decline in HC growth rates as the curve radius increases beyond 1000 m. However, on tight curves with very small radii (e.g., below 750 m), wear caused by the friction becomes a more dominant damage mechanism that suppresses the RCF by removing the surface-initiated cracks before they have a chance to grow. This interplay explains the initial rise of the HC growth rate as the radius increases within 750 m.

Overall, the HC growth rates of R260 rails in the Belgian rail network are in the range of 0.4–1.5 mm/100 MGT across the curve radii. These values are generally comparable to, but somewhat lower than, the growth rates reported for the DB network, which ranges from 0.8 to 2.0 mm/100 MGT [21]. Several factors may account for this deviation, including differences in the dataset size (212 curves in the current analysis versus 47 curves in the DB study) and variations in rolling stock characteristics. Belgium started the modernisation of its rolling stock in 2016, whereas Germany began this process several years earlier. In addition, some statistical uncertainty in the growth rate calculations may occur, influenced by factors such as cant deficiency and the accuracy limitations of ECT systems.

3.2. HC growth versus annual train load and UIC class

Fig. 5a shows the relationship between the HC growth rates and annual tonnage, based on data from all the 212 curves. The curves were grouped by their crack growth rates per 100 MGT, and the average annual tonnage was then calculated for each group. A counterintuitive trend is observed: HC growth rates are higher on railway lines with lower annual tonnage. This observation provided the basis for further analysis, where the growth rates were subdivided according to the different UIC classes, expressed as a function of annual train load. A similar observation was reported for rail wear in [33], where the wear rates were found to be higher on lower-loaded lines. Since HC growth is expressed in mm/100 MGT, tracks with lower annual tonnage take longer service time to reach the same cumulative load. This suggests that time-related factors, such as fluid pressurisation within cracks [25] or crack-tip corrosion [36], play a significant role in HC development. Therefore, annual train load and the corresponding service time should be considered as a critical factor for HC, together with the cumulative traffic load.

To further investigate this phenomenon, Fig. 5b presents the HC growth rates across different UIC line classes. The results show that HC growth is more pronounced on low-loaded lines. Specifically, the growth rate on UIC4 lines is approximately twice that of UIC3, and about half that of UIC5. These findings highlight the importance of annual load and service time in influencing HC development. In addition, Fig. 5b shows that for both UIC3 and UIC4 lines, the fastest HC growth occurs on curves with radii between 750 and 1250 m, consistent with the trends in Fig. 4.

3.3. HC growth per year

In the analyses above, the HC growth rate was expressed in mm/100 MGT, as defined in Equation (3). In this section, the HC growth rate is evaluated in mm/year since the rail installation, based on Equation (4). The wear induced by grinding is not considered in this analysis, as the field measurements indicate that the curves with HCs show an average wear rate similar to that measured in 2012 before the implementation of the preventive grinding strategy. Fig. 6 shows the annual HC growth rates per UIC group as a function of curve radius. The overall trend in relation to radius is similar to that observed in mm/100 MGT: annual HC growth rate initially increases with curve radius, reaching a peak in the range of 750–1250 m, and then decreases with further increases in radius.

When evaluated on a time basis (mm/year), HC growth rates increase on higher-loaded lines, in contrast to the trend observed when

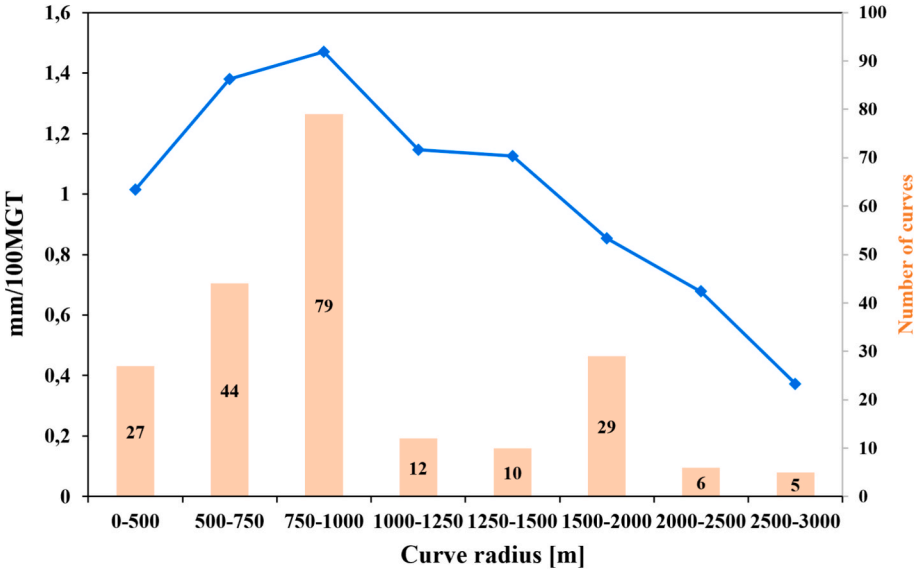

Fig. 4. HC growth rates of R260 rails as a function of the curve radius measured in 2019.

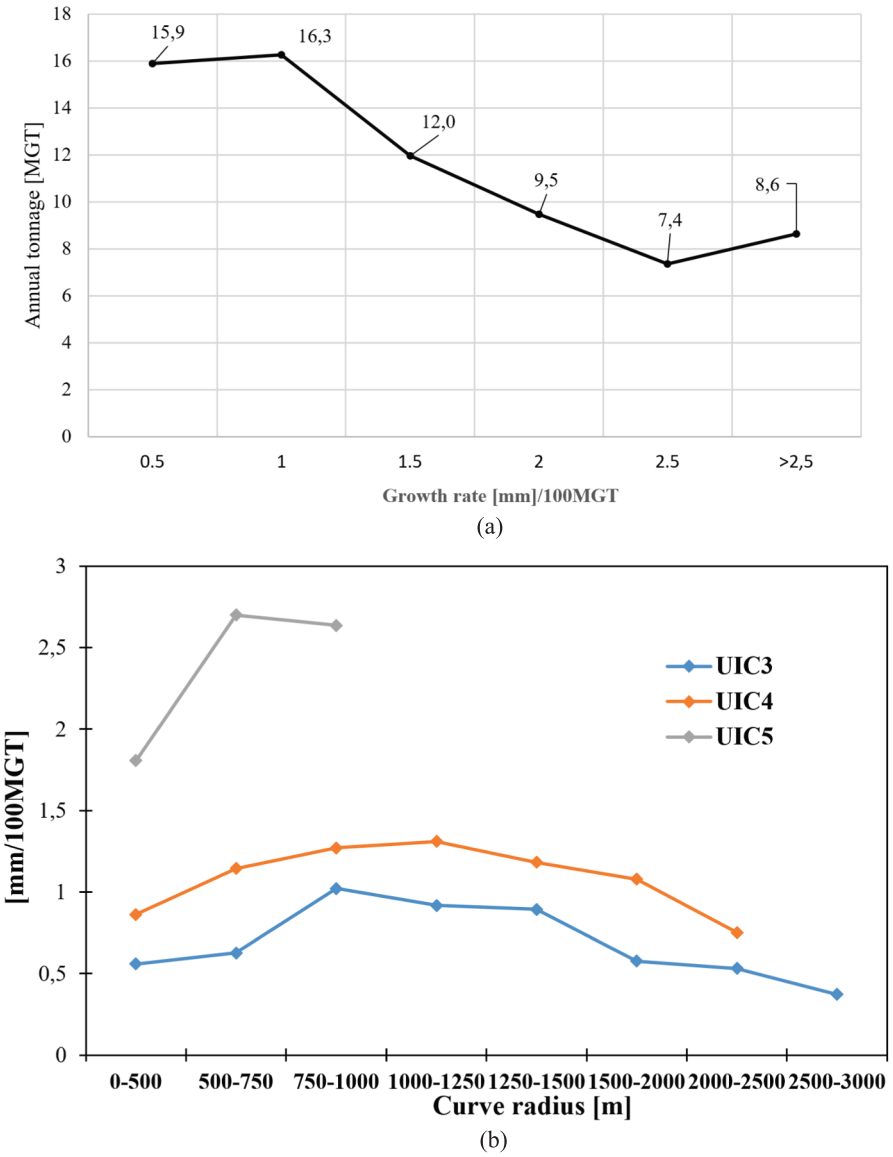

Fig. 5. The effect of annual train load on HC growth. (a) HC growth in relation to average annual tonnage; (b) HC growth for UIC3, UIC4 and UIC5 classes.

normalised by tonnage (mm/MGT). Higher daily loads result in greater HC growth per year as expected, but the rate of increase is not proportional to the increase in daily load. For example, on curves with radii between 750 and 1000 m, the HC growth rate rises only slightly, from 0.14 mm/year on UIC4 lines to 0.16 mm/year on UIC3 lines, despite the nearly doubled daily load. This indicates that traffic load alone does not fully explain the variation in HC growth. Other contributing factors, such as fluid pressurisation within cracks and crack-tip corrosion, as discussed in Section 3.2, likely play a significant role in driving crack development.

3.4. The relationship between HC growth and rail wear rate

This section presents the field statistical data to illustrate the competing mechanisms between rail wear and RCF, as shown in Fig. 7. The analysis focuses on rail wear measured at 45° [33], including both the natural wear caused by wheel-rail interaction and corrosion, and the artificial wear from the preventive grinding. Wear rate is calculated as the amount of rail material (in millimetres) removed per 100 MGT of traffic.

Fig. 7a shows that the rail wear rate per tonnage for UIC3 and UIC4 lines generally decreases linearly with increasing curve radius. This observation supports the claim made in Section 3.1 that tighter curves have higher frictional energy. Notably, the wear rate on UIC4 lines is approximately 50 % higher than that on UIC3 lines. In curves with radii smaller than 750 m, the average wear rate significantly suppresses the HC development, as material removal prevents crack initiation and growth. In contrast, on curves with radii between 750 m and 1500 m, the average HC growth rate exceeds the average wear rate, indicating that RCF becomes the dominant damage mechanism in this range. By comparing HC and wear rates for curves with radii below 750 m and those between 750 m and 1500 m, it can be seen that artificially increasing the wear rate, e.g., through preventive grinding, can substantially reduce HC growth.

Beyond a radius of 1500 m, the HC growth rate decreases more sharply than the wear rate. This behaviour is likely due to the formation mechanism of HCs, which require wheel–rail contact stresses to exceed a critical threshold that leads to ratcheting and subsequent crack initiation [12]. For example, for UIC3 lines, on curves with radii larger than approximately 1500 m, contact stresses may fall below this threshold, resulting in reduced HC formation. Unlike HC, rail wear does not have a defined initiation threshold and therefore decreases more gradually with

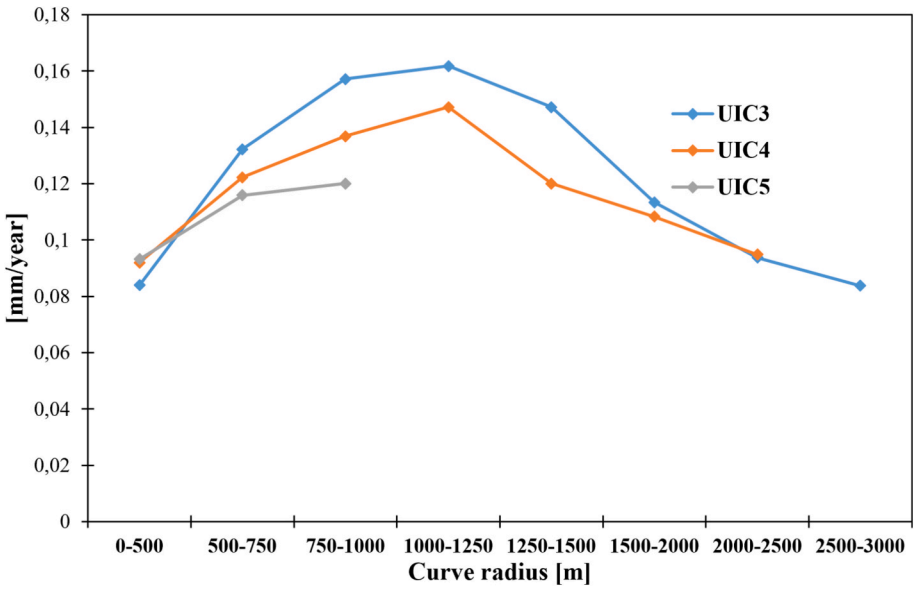

Fig. 6. HC growth in mm per year as a function of curve radius and track classes.

increasing radius.

Fig. 7b shows the annual rail wear and HC growth rates as a function of curve radius, showing a trend similar to the tonnage-based analysis. It can be seen that the average HC growth rates per year are comparable for UIC3 and UIC4 lines. This suggests that, when considered on a time basis, HC defects on low-loaded tracks can develop at rates similar to those on more high-loaded lines. This finding has important implications for the design of preventive grinding strategies. For low-loaded tracks, the annual increase in wear is less effective in suppressing HCs compared to that in high-loaded lines. As a result, even tight curves on low-loaded tracks may be vulnerable to HC formation. This can be supported by the data in Fig. 7b that the HC growth rate for curves with radii below 500 m, is higher on UIC4 than on UIC3 lines.

4. Estimation of MWR for HC treatment

Preventive grinding strategies have been implemented across European railway networks to control RCF defects. The intervals between successive grinding campaigns have been typically determined based on cumulative tonnage, with typical values ranging from 15 to 25 MGT. However, as shown in the analysis above, HC growth is influenced not only by cumulative tonnage but also by the annual traffic load and time. In this section, we first evaluate the effectiveness of the current grinding policy in mitigating HC development. Afterwards, we propose a new approach for defining the optimal grinding strategy, referred to as the MWR, which is derived from the statistical data of the natural wear rates and HC growth rates across the Belgian railway network. The analysis focuses on UIC3, UIC4 and UIC5 line classes, which represent the majority of the rail networks in Belgium.

4.1. Evaluation of the effectiveness of the current grinding policy

In Belgium, Infrabel has implemented a preventive grinding interval of 25 MGT for curves on UIC1-6 lines since 2016. The material removal per grinding campaign is approximately 0.25 mm, corresponding to an artificial wear rate of 1.0 mm/100 MGT. Under this grinding policy, the total wear rates are calculated per UIC-class using the equations below.

$$W_{tot} = W_n + W_a = W_n + 100G_d/G_i \quad (6)$$

where W_{tot} is the total wear rate in mm/100 MGT; W_n is the natural wear rate caused by traffic load and corrosion; W_a is the artificial wear rate introduced from preventive grinding; G_d is the grinding depth per interval (0.25 mm); G_i is the traffic load every grinding interval (25 MGT). Given that head checks exhibit the fastest growth in curves with radii between 750 m and 1500 m, the calculations in Table 1 are limited to this radius range. The corresponding natural, artificial, and total wear rates for each UIC class are summarised in Table 1.

The results in Table 1 indicate that natural wear per 100 MGT is significantly higher on annually lower-loaded lines. Since the same grinding interval is applied across all UIC classes based on cumulative tonnage, the proportion of artificial wear relative to total wear is considerably lower for low-loaded lines than for high-loaded ones. For example, artificial wear accounts for approximately 142 % of the natural wear on UIC3 lines, while it represents only about 42 % on UIC5 lines. When considered from a time-based perspective, this implies that grinding on UIC3 lines occurs roughly once per year (25 MGT/22 MGT≈1), whereas for UIC5 lines, the same grinding interval corresponds to approximately one grinding campaign every five years (25 MGT/4.6 MGT≈5) due to lower annual tonnage.

Statistical data show that in 2016, about 375 km of the Belgian rail network were affected by HCs. By 2023, this number decreased to around 125 km, representing a substantial 70 % reduction. This result suggests that the current preventive grinding strategy has been generally effective in reducing the overall extent of HC-affected tracks. However, a more detailed analysis reveals that despite the reduction in affected track length, the average HC growth rates in 2023 have increased compared to 2016, as shown in Table 2. While this increase is insignificant for UIC3 (3 %), it is very pronounced in low-loaded lines, reaching up to 76 % and 200 % for UIC4 and UIC5, respectively. These findings indicate that a grinding interval of 25 MGT is sufficient for managing HC development on high-loaded lines like UIC3, but is inadequate for lower-loaded lines like UIC4 and UIC5. Furthermore, the data suggest that when grinding fails to fully remove existing HCs, the remaining defects may grow at an accelerated rate. More field observations and studies could be performed to further verify this finding.

4.2. MWR for HC treatment in Belgium

The current grinding policy, which is solely based on accumulated tonnage, has limitations in effectively mitigating HCs, particularly on lower-loaded lines. This is mainly because it does not account for the influence of annual load and time-related factors on HC growth. Ideally, artificial wear introduced through preventive grinding should be pre-

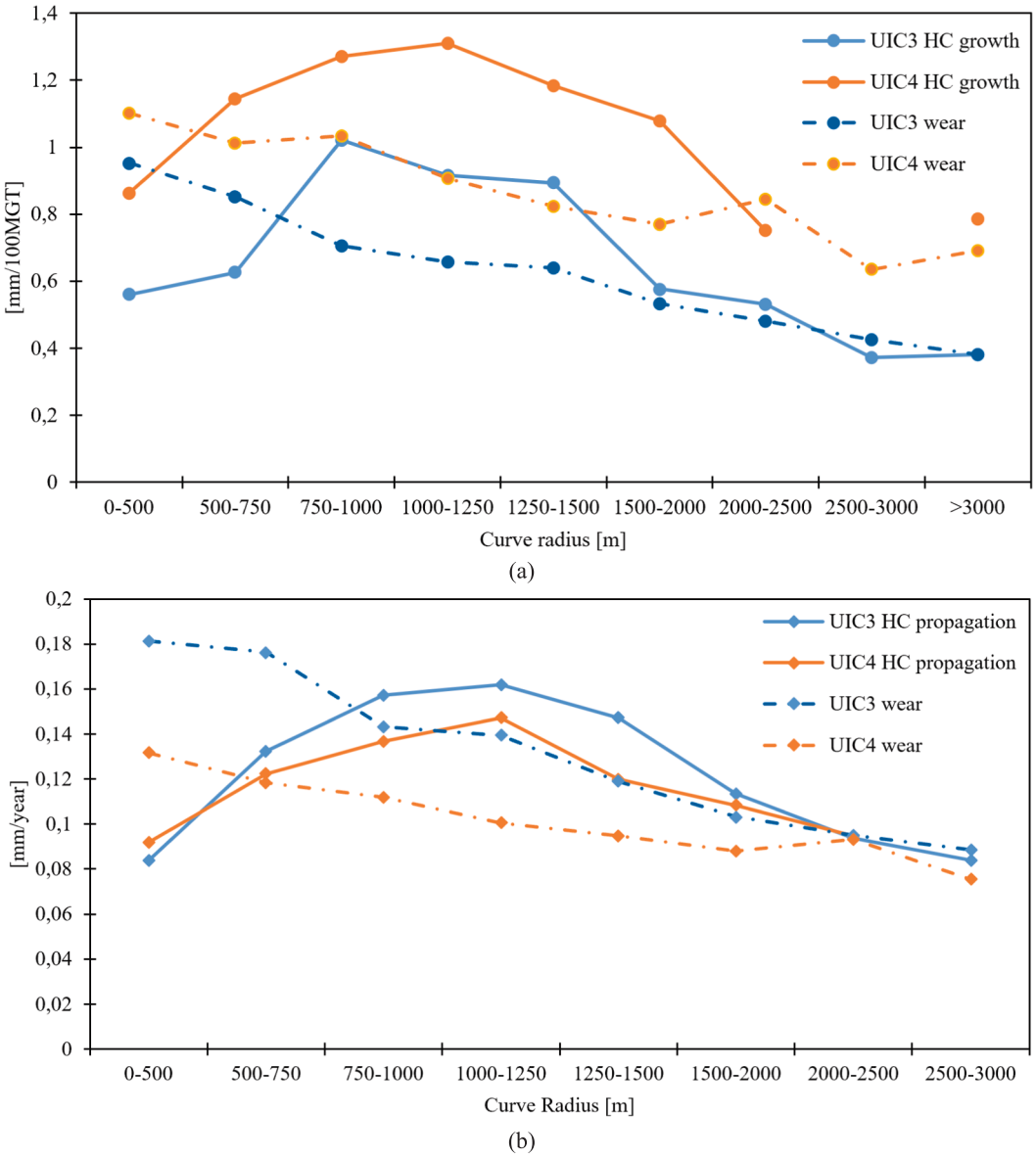

Fig. 7. The relationship between HC growth and wear rates. (a) HC growth and rail wear per tonnage as a function of curve radius; (b) HC growth and rail wear per year as a function of curve radius.

Table 1
The wear rate per UIC class based on the current grinding policy. The natural wear data was from [33].

UIC-Class	Annual load [MGT]	Natural wear at 45° [mm/100MGT]	Artificial wear per grinding interval [mm/25 MGT]	Total wear rate [mm/100 MGT]	Artificial wear/total wear
UIC3	22	0.7	0.25	1.7	142 %
UIC4	11	0.9	0.25	1.9	111 %
UIC5	4.6	2.4	0.25	3.4	42 %

Table 2
HC growth rate in 2023 with the current grinding policy.

UIC-Class	Annual load [MGT]	HC growth rate in 2019 without grinding [mm/100MGT]	HC growth rate in 2023 with grinding [mm/100MGT]	Increase in growth rate from 2019 to 2023
UIC3	22	0.9	1.0	3 %
UIC4	11	1.3	2.2	76 %
UIC5	4.6	2.7	8.0	200 %

cisely calibrated to remove existing HCs. To achieve this balance, the concept of the MWR is introduced, which defines the optimal amount of material removal required to eliminate HCs without causing unnecessary rail material loss. The MWR can be calculated as the sum of the natural wear rate and HC growth rate, as follows:

$$MWR = W_n + W_a = W_n + Dh \tag{7}$$

Where Δh is the HC growth rate in mm/100 MGT, which is obtained from the statistical data. Then we can calculate the required grinding interval based on a grinding depth of 0.25 mm as follows,

$$G_i = 100G_d/Dh \tag{8}$$

Table 3 summarizes the calculated MWR and the corresponding grinding interval for the UIC3, UIC4, and UIC5 lines. When compared with the

Table 3
The calculated MWR as the sum of the natural wear rate and HC growth rate.

UIC-Class	Annual load [MGT]	Natural wear at 45° [mm/100MGT]	HC growth rate in 2019 without grinding [mm/100MGT]	MWR [mm/100MGT]	Proposed grinding interval [MGT]
UIC3	22	0.7	0.9	1.6	27.8
UIC4	11	0.9	1.3	2.2	19.2
UIC5	4.6	2.4	2.7	5.1	9.2

values in Table 2, it is found that for UIC3, the MWR is slightly lower than the total wear rate, and the proposed grinding interval of 27.8 MGT is higher than the current strategy of 25 MGT. This suggests that the existing grinding policy is adequate for controlling HC growth on UIC3 lines. However, for lower-loaded UIC4 and UIC5 curves, the MWR is significantly larger than the total wear rate, indicating that the current grinding interval of 25 MGT is too large to effectively manage HC development. Based on the MWR analysis, the optimal grinding intervals should be approximately 19.2 MGT for UIC4 and 9.2 MGT for UIC5. The insufficient grinding frequency on these lines may explain the accelerated HC growth rates observed in Table 2. These findings highlight the need for different grinding strategies that consider both cumulative tonnage and annual traffic load, particularly for low-loaded tracks.

5. Conclusions

This paper investigates the HC growth rate through a statistical analysis of data from the Belgian railway network. Extensive field data were collected and analysed from 212 curved track sections with different track radii and annual traffic loads. Crack depths were mainly measured using the eddy current testing. The HC growth rates were then compared with the corresponding rail wear rates to better understand the interplay between wear and HC. Afterwards, the effectiveness of the current grinding policy in controlling HC development has been evaluated. Based on the measured HC and wear rates, the MWR has been proposed to define the optimal grinding interval for different UIC line classes. The main conclusions have been summarised as follows.

(1) The tracks with radii between 750 and 1000 m have the highest HC growth rate, reaching about 1.5 mm/100 MGT, and the largest occurrence probability of around 25 %. On curves with radii less than 750 m, the rail wear becomes a more dominant damage mechanism, significantly suppressing HC growth.
(2) A counterintuitive trend is observed that HC growth per tonnage is higher on railway lines with annually lower-loaded lines, consistent with the trend observed in rail wear rates. This result suggests the importance of time on rail damage development, together with the traffic loads.
(3) The MWR has been calculated as the sum of the natural wear rate and HC growth rate per UIC class in the Belgian railway network, and the corresponding grinding intervals are 27.8, 19.2, and 9.2 MGT for UIC3, UIC4, and UIC5, respectively.
(4) The current preventive grinding strategy in Belgium, 0.25 mm/25MGT for all UIC curves, has been generally effective in reducing the overall extent of HC-affected tracks. However, it is insufficient for low-loaded tracks, including UIC4 and UIC5, and may accelerate the HC growth rate.

Overall, this work contributes to a better understanding of the HC growth process and provides valuable insights into the predictive maintenance strategies in the treatment of rail RCF defects. In future work, the statistical analysis on other railway networks could be performed, and the corresponding MWR could be obtained and compared to this work. Besides, it is interesting to investigate the acceleration mechanisms for HC crack growth by grinding for low-loaded track in future work.

CRediT authorship contribution statement

Tim Vernaillen: Writing – original draft, Visualization, Validation, Resources, Methodology, Investigation, Funding acquisition, Formal analysis, Data curation, Conceptualization. **Pan Zhang:** Writing – review & editing, Writing – original draft, Visualization, Supervision, Methodology, Investigation, Formal analysis. **Alfredo Núñez:** Writing – review & editing, Visualization, Supervision, Project administration, Methodology, Investigation, Funding acquisition, Formal analysis, Conceptualization. **Rolf Dollevoet:** Writing – review & editing, Supervision, Resources, Project administration. **Zili Li:** Writing – review & editing, Validation, Supervision, Resources, Methodology, Investigation, Formal analysis, Conceptualization.

Declaration of competing interest

The authors declare that they have no known competing financial interests or personal relationships that could have appeared to influence the work reported in this paper.

Acknowledgment

This work is partly funded by Infrabel.

Data availability

Data will be made available on request.

References

[1] E.E. Magel, Rolling contact fatigue: a comprehensive review, (2011).
[2] Muhamedsalih Y, Hawksbee S, Tucker G, Stow J, Burstow M. Squats on the Great Britain rail network: possible root causes and research recommendations. Int J Fatigue 2021;149:106267.
[3] Ma X, Yin W, Wang Y, Liu L, Wang X, Qian Y. Fatigue failure analysis of U75V rail material under I+ II mixed-mode loading: characterization using peridynamics and experimental verification. Int J Fatigue 2024;185:108371.
[4] Cannon D, Edel KO, Grassie S, Sawley K. Rail defects: an overview. Fatigue Fract Eng Mater Struct 2003;26:865–86.
[5] Zhou Y, Han Y, Mu D, Zhang C, Huang X. Prediction of the coexistence of rail head check initiation and wear growth. Int J Fatigue 2018;112:289–300.
[6] M. Ph Papaelias, C. Roberts, C.L. Davis, A review on non-destructive evaluation of rails: State-of-the-art and future development, Proc Inst Mech Eng, F: J Rail Rapid Transit, 222 (2008) 367-384.
[7] Zhou Y, Zheng X, Jiang J, Kuang D. Modeling of rail head checks by X-ray computed tomography scan technology. Int J Fatigue 2017;100:21–31.
[8] Zoeteman A. Life cycle cost analysis for managing rail infrastructure: concept of a decision support system for railway design and maintenance. Eur J Transp Infrastruct Res 2001;1.
[9] Ekberg A, Åkesson B, Kabo E. Wheel/rail rolling contact fatigue–probe, predict, prevent. Wear 2014;314:2–12.
[10] Meghoe A, Jamshidi A, Loendersloot R, Tinga T. A hybrid predictive methodology for head checks in railway infrastructure. Proc Inst Mech Eng, F: J Rail Rapid Transit 2021;235:1312–22.
[11] R.P. Dollevoet, Design of an Anti Head Check profile based on stress relief, (2010).
[12] R. Dollevoet, Z. Li, O. Arias-Cuevas, A method for the prediction of head checking initiation location and orientation under operational loading conditions, Proc Inst Mech Eng, F: J Rail Rapid Transit, 224 (2010) 369-374.
[13] Tsujie M, Miura M, Chen H, Terumichi Y. A study on the initiation of head check of the low rail using multibody dynamics. Wear 2019;436:202989.
[14] Nezhad MS, Larsson F, Kabo E, Ekberg A. Finite element analyses of rail head cracks: predicting direction and rate of rolling contact fatigue crack growth. Eng Fract Mech 2024;310:110503.
[15] Xie Y, Ding H, Shi Z, Meli E, Guo J, Liu Q, et al. A novel prediction method for rolling contact fatigue damage of the pearlite rail materials based on shakedown limits and rough set theory with cloud model. Int J Fatigue 2025;190:108654.
[16] Takikawa M, Iriya Y. Laboratory simulations with twin-disc machine on head check. Wear 2008;265:1300–8.
[17] Ren F, Yang Z, Li Z. Experimental and numerical investigation into rolling contact fatigue crack initiation on the V-Track test rig. Eng Fail Anal 2025;170:109206.

[18] Nguyen BH, Al-Juboori A, Zhu H, Zhu Q, Li H, Tieu K. Formation mechanism and evolution of white etching layers on different rail grades. Int J Fatigue 2022;163:107100.
[19] Hiensch M, Steenbergen M. Rolling contact fatigue on premium rail grades: damage function development from field data. Wear 2018;394:187–94.
[20] Zhou Y, Wang S, Wang T, Xu Y, Li Z. Field and laboratory investigation of the relationship between rail head check and wear in a heavy-haul railway. Wear 2014;315:68–77.
[21] Heyder R, Brehmer M. Empirical studies of head check propagation on the DB network. Wear 2014;314:36–43.
[22] Donzella G, Faccoli M, Mazzù A, Petrogalli C, Roberti R. Progressive damage assessment in the near-surface layer of railway wheel–rail couple under cyclic contact. Wear 2011;271:408–16.
[23] Pun CL, Kan Q, Mutton PJ, Kang G, Yan W. Ratcheting behaviour of high strength rail steels under bi-axial compression–torsion loadings: experiment and simulation. Int J Fatigue 2014;66:138–54.
[24] Bogdański S, Lewicki P. 3D model of liquid entrapment mechanism for rolling contact fatigue cracks in rails. Wear 2008;265:1356–62.
[25] Fletcher D, Hyde P, Kapoor A. Modelling and full-scale trials to investigate fluid pressurisation of rolling contact fatigue cracks. Wear 2008;265:1317–24.
[26] Zhang S, Zhao H, Ding H, Lin Q, Wang W, Guo J, et al. Effect of vibration amplitude and axle load on the rail rolling contact fatigue under water condition. Int J Fatigue 2023;167:107329.
[27] Smallwood R, Sinclair J, Sawley K. An optimization technique to minimize rail contact stresses. Wear 1991;144:373–84.
[28] Fletcher D, Beynon J. The effect of intermittent lubrication on the fatigue life of pearlitic rail steel in rolling-sliding contact. Proc Inst Mech Eng, F: J Rail Rapid Transit 2000;214:145–58.
[29] Grassie SL. Rolling contact fatigue on the British railway system: treatment. Wear 2005;258:1310–8.
[30] Kalousek J. Achieveing a balance: the'magic'wear rate. Railway Track & Structures 1997.
[31] E. Magel, J. Kalousek, P. Sroba, Chasing the magic wear rate, in: Proceedings of the second international conference on railway technology: research, development and maintenance, Paper, 2014.
[32] Rajamäki J, Vippola M, Nurmikolu A, Viitala T. Limitations of eddy current inspection in railway rail evaluation. Proc Inst Mech Eng, F: J Rail Rapid Transit 2018;232:121–9.
[33] Vernaillen T, Wang L, Núñez A, Dollevoet R, Li Z. Rail wear rate on the Belgian railway network–a big-data analysis. Int J Rail Transp 2023:1–16.
[34] Donzella G, Mazzù A, Petrogalli C. Competition between wear and rolling contact fatigue at the wheel—rail interface: some experimental evidence on rail steel. Proc Inst Mech Eng, F: J Rail Rapid Transit 2009;223:31–44.
[35] Wang H, Wang W, Han Z, Wang Y, Ding H, Lewis R, et al. Wear and rolling contact fatigue competition mechanism of different types of rail steels under various slip ratios. Wear 2023;522:204721.
[36] Wang K, Bai T, Xu J, Zhu H, Qian Y, Wang X, et al. Investigation into the mechanisms of Corrosion-Induced rolling contact fatigue crack initiation and propagation in pearlitic rails. Eng Fail Anal 2024;163:108614.